



Nanourchin-like Uricase-Poly(L-proline) Conjugate with Retained Enzymatic Activity, Mitigated Immunogenicity, and Sustained Efficacy Upon Repeated Administrations

Ruichi Zhao⁺, Yangming Zhang⁺, Banlai Ruan, Hairuo Zhang, Niannian Lv, Jiayi Li, Yuhe R. Yang,* Xiaozhou Luo,* and Hua Lu*

Abstract: The poor half-life and strong immunogenicity of proteins such as uricase (UOx), a therapeutic enzyme for chronic refractory gout and hyperuricemia, are pressing clinical challenges. Although conjugation of poly(ethylene glycol) (PEGylation) of UOx can improve the pharmacokinetics, preexisting or induced anti-PEG antibodies, which lead to accelerate blood clearance (ABC) and reduced response rate, have been a major clinical hurdle. Herein, we report the facile “grafting-from” preparation of a nanourchin-like uricase-poly(L-proline) conjugate, namely UOx-PLP, with high grafting-density, enhanced thermal, lyophilization, freeze-thaw, and proteolytic stability. Through a transient preblocking strategy in the synthesis, the UOx-PLP overcomes activity loss and retains ~82 % enzyme activity. In Sprague-Dawley rats, UOx-PLP stimulates minimum complement activation and anti-UOx antibodies. Unlike PEG-UOx gave a significantly reduced half-life after repetitive administrations, UOx-PLP shows no sign of ABC effect. Moreover, the half-life of UOx-PLP remain almost unchanged when cross-administrated to rats previously received PEG-UOx and with high titers of anti-UOx antibodies. Finally, UOx-PLP shows minimum loss of efficacy after five straight administrations in a UOx knock-out hyperuricemia mice model, whereas PEG-UOx experiences sharp loss of efficacy upon the same treatment. Overall, the simple preparation and outstanding nonclinical results highlight the enormous potential of UOx-PLP for future clinical translation.

Introduction

Hyperuricemia and gout are complicated, painful, and prevalent diseases characterized by excessive buildup of uric acid in the body.^[1] Currently, there are over 55 million patients suffer from gout worldwide, and the population of

hyperuricemia far exceeds 200 million.^[2] Uric acid is the end product of purine metabolism, and due to its low solubility in water, any excess production of uric acid or failure in its excretion can lead to hyperuricemia or the formation of monosodium urate crystals.^[3] A functional enzyme known as uricase (UOx), which converts the poorly soluble uric acid into the more soluble and easier-to-excrete allantoin, is present in most organisms but not certain primates, including human.^[4] To date, the enzyme replacement therapy (ERT) is a proven treatment of the above diseases by supplementing exogenous UOx to degrade excessive uric acid in the body.^[5]

Rasburicase, a recombinant *Aspergillus flavus* uricase was approved for primary treatment of hyperuricemia during chemotherapy by the FDA in 2002.^[6] However, the high immunogenicity of Rasburicase makes it an unlikely choice for the treatment of chronic hyperuricemia and gout. Antibody responses were observed in 64 % of volunteers within 1 to 6 weeks after the initial course, with persistent antibodies for over 1 year.^[7] To address these clinical challenges, a PEGylated pig-baboon chimeric uricase called Pegloticase (KRYSTEXXA[®]) with prolonged half-life and reduced immunogenicity has been developed and approved by the FDA for the treatment of chronic refractory gout in 2010.^[8] Despite significant improvements in pharmacokinetics, still, to Pegloticase was issued a black box warning by the FDA and discontinued in Europe due to low response rate and strong immunogenicity raised by antidrug antibodies.^[9] Specifically, 92 % of patients developed anti-

[*] R. Zhao,⁺ H. Zhang, H. Lu

Beijing National Laboratory for Molecular Sciences, Center for Soft Matter Science and Engineering, Key Laboratory of Polymer Chemistry and Physics of Ministry of Education, College of Chemistry and Molecular Engineering, Peking University, Beijing 100871, People's Republic of China
E-mail: chemhualu@pku.edu.cn

Y. Zhang,⁺ B. Ruan, X. Luo

Shenzhen Key Laboratory for the Intelligent Microbial Manufacturing of Medicines, Key Laboratory of Quantitative Synthetic Biology, Center for Synthetic Biochemistry, Shenzhen Institute of Synthetic Biology, Shenzhen Institutes of Advanced Technology, Chinese Academy of Sciences, Shenzhen, 518055, People's Republic of China
E-mail: xz.luo@siat.ac.cn

N. Lv, J. Li, Y. R. Yang

CAS Key Laboratory of Nanosystem and Hierarchical Fabrication, National Center for Nanoscience and Technology of China, CAS, Beijing, 100190, China
E-mail: yangyh@nanoctr.cn

N. Lv, J. Li, Y. R. Yang

University of Chinese Academy of Sciences, Beijing 100049, China

[†] Equally contributed to this work

bodies against Pegloticase, and 42 % developed antibodies against PEG.^[10] The production of anti-PEG antibodies is associated with a decrease in the efficacy of Pegloticase over time and an increase in the incidence of infusion reactions.^[11] In patients with high titers of PEG antibodies, approximately 50 % experienced an infusion reaction during subsequent administration (26 % severe, 6.5 % life-threatening allergic reactions).^[12] More concerning is the prevalent and significantly boosted anti-PEG antibodies in healthy populations after receiving two or more PEGylated lipid nanoparticle (PEG-LNP) mRNA vaccines during the COVID-19 pandemic, which jeopardizes the use of any other PEGylated drugs for patients with high preexisting anti-PEG antibodies.^[13]

To address these unmet clinical needs and challenges, various synthetic polymers and recombinant polypeptides (to name a few: PAS, EK, XTEN, ELP, POEGMA, zwitterionic polymers, polyglycerol, polyoxazoline, polypept(o)ides such as polysarcosine, polysulfoxide, poly(*N*-oxide), *etc.*) have been fused/conjugated to therapeutic proteins for reduced immunogenicity, including UOx.^[14] Nanogels and nanoparticles encapsulating UOx are also developed to give reduced immunogenicity of UOx.^[15] More recently, UOx-loaded red blood cells or LNP-delivered UOx mRNA were used.^[16] However, fusion and the so-called “grafting-to” approaches often afforded low or modest degree of modifications, which is suboptimal to fully shield the immunogenic epitopes of UOx.^[17] On the other hand, conventional grafting-to strategy suffers low grafting efficiency due to steric hindrance, and there was a dilemma that the higher the grafting density, often the lower the activity. To this end, a simple strategy for high modification degree, complete epitope masking, yet without compromising the enzymatic activity, is highly desirable toward next-generation UOx-based therapeutics.

Herein, we report the “grafting-from” preparation of uricase-poly(*L*-proline) conjugates, namely UOx-PLP, through ultrafast in situ protein-initiated ring-opening polymerization (ROP) of proline *N*-carboxyanhydride (ProNCA). The facile method yields nanourchin-like conjugates ~20 nm in size, featuring in UOx in the core and a high grafting-density protecting layer of neutral, water-soluble PLP bearing the rigid polyproline II (PPII) helix on the surface (Figure 1A). By applying a transient preblocking strategy during the synthesis, the obtained UOx-PLP overcomes the activity loss and retains ~82 % enzyme activity of UOx with enhanced thermal, lyophilization, freeze-thaw, and proteolytic stability in vitro compared to the PEG-UOx control. In Sprague-Dawley rats, UOx-PLP stimulates minimum complement activation, and decreases titers in anti-UOx and anti-PEG antibodies for more than 250 and 30 times, respectively. Unlike PEG-UOx gave a significantly reduced half-life after repetitive administrations, UOx-PLP showed no sign of ABC effect. Moreover, the pharmacokinetics (PK) of UOx-PLP remain almost unchanged when cross-administrated to rats previously received PEG-UOx and with high titers of both anti-UOx and anti-PEG antibodies. Finally, UOx-PLP shows minimum loss of efficacy after five straight administrations in a UOx knock-out (*Uox-*

KO) hyperuricemia mice model, whereas PEG-UOx experiences sharp loss of efficacy upon the same treatment.

Results and Discussion

Grafting-from Synthesis and Characterizations of UOx-PLP

Previously, we developed a simple, water-assisted ultrafast controllable ROP of ProNCA to prepare PLP, which was later widely used by others owing to the robustness and simplicity of the method.^[18] Importantly, the protocol allowed the use of proteins, with the solvent-exposed lysine ϵ -NH₂, as initiators for the ROP of ProNCA without the need of pre-modification. To make UOx-PLP, ProNCA in acetonitrile (ACN) was mixed with UOx purified by affinity chromatography (Figure S1) in phosphate buffer and agitated gently. Immediate release of CO₂ bubble was observed, which typically finished within 5 min (Figure 1A). The size of the conjugated PLP could be controlled by the feeding UOx and ProNCA ratio. However, substantially reduced enzyme activity was found for the product (Figure 1B), likely due to undesirable block of catalytic center by the grafted PLP. To circumvent this problem, a transient preblocking strategy was applied, namely by adding a competitive inhibitor of uric acid, xonic acid potassium salt, to the polymerization solution, which was easily removable during the size exclusion chromatography (SEC) purification. In this generation-two protocol, the prepared UOx-PLP conjugate was able to preserve ~82 % activity of the pristine enzyme (Figure 1B). The purified UOx-PLP revealed a significantly shifted unimodal peak to the higher molecular-weight (M_n) region in SEC (Figure 1C) and dynamic light scattering (DLS) measurement gave a hydrodynamic diameter of ~18.9 nm for UOx-PLP, roughly ~10 nm greater than the wild type UOx (Figure 1D). Sodium dodecyl sulfate polyacrylamide gel electrophoresis (SDS-PAGE) analysis of the product gave a smeared band shifting to the upper M_n region (Figure S2). These data collectively confirmed the successful PLP conjugation. The overlay of SEC traces of three different batches showed almost identical retention time and peak shape of the products, which also displayed comparable enzymatic activities, underlying the reproducibility of the method (Figure S3), underscoring the excellent reproducibility of the synthetic method. Cryo-electron microscopy (cryo-EM) comparison of UOx and UOx-PLP indicated that the higher-ordered structure of UOx was not affected by PLP conjugation (Figure 1E and Figure S4). Direct observation of the conjugated PLP by Cryo-EM, unfortunately, was unsuccessful, perhaps a result of the small diameter of outstretched PPII helix (~7.36 Å) and low resolution of the PLP strand.^[19] Due to the extensive modification of PLP, circular dichroism (CD) spectroscopy of the purified product exhibited typical pattern of PPII helix masking the original pattern of UOx (Figure S5). A PEG-UOx conjugate was also synthesized through random grafting-to strategy using amine-NHS chemistry for comparison (Scheme S1). PEG of 10 kDa was selected for conjugation as this was the M_n used in Pegloti-

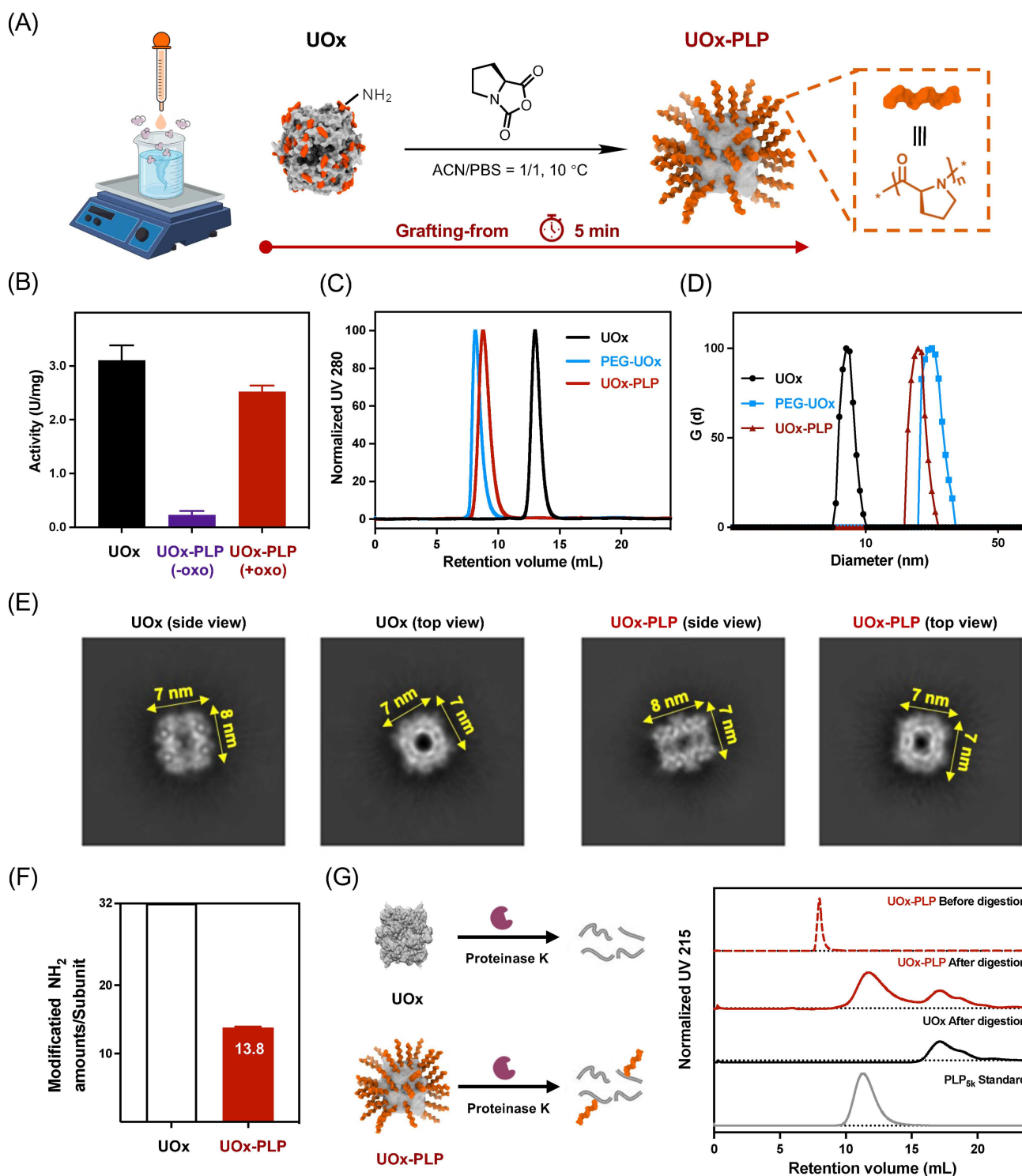


Figure 1. Synthesis and characterization of UOx-PLP and PEG-UOx. (A) Synthetic Scheme of UOx-PLP using the grafting-from approach. (B) Enzymatic activity of UOx-PLP prepared without or with addition of xonic acid potassium salt (oxo). (C) Size exclusion chromatography (SEC), (D) dynamic light scattering (DLS) of UOx, UOx-PLP, and PEG-UOx. G(d) represents the size distribution function based on the number of particles. (E) Representative 2D class averages of UOx and UOx-PLP particles, with double arrows and values indicating size measurements in various directions. For each particle, the side view is on the left, while the top view is on the right. (F) Degree of PLP modification determined by the chemoselective assay for secondary amines. (G) Scheme of UOx and UOx-PLP by proteinase K digestion (left) and the SEC analysis of the degraded products (right).

case. SEC, DLS, and SDS-PAGE analyses all suggested that PEG-UOx was slightly larger in size than UOx-PLP (Fig-

ure 1C–D and Figure S2), a result we attributed to the high M_n and extended conformation of PEG.

To determine the degree of PLP modification in UOx-PLP, we employed a triazene chemistry developed by Raj et al. that could selectively quantify the amount of secondary amines using UV/Vis spectrometry.^[20] Briefly, the terminal secondary amine of PLP chains reacted with arene diazonium ions rapidly to generate a stable triazene with characteristic absorbance at 340 nm (Scheme S2 and Figure S6). Using this method, UOx-PLP was calculated to bear approximately ~13.8 PLP chains per UOx subunit after deduction of background absorption from UOx (Figure 1F). The degree of modification for both PEG-UOx and UOx-PLP was also determined indirectly by measuring the free primary amines of UOx before and after polymer conjugation using trinitrobenzene sulfonic acid (TNBS). As shown in Figure S7, approximately 26% and 33% of the primary amines were modified with PEG and PLP, respectively. This suggests that, theoretically, each subunit of UOx is conjugated with about 8.1 PEG chains for PEG-UOx and 10.6 PLP chains for UOx-PLP. The 8.1 PEG chains per subunit in PEG-UOx align well with the 9–10 PEG chains per subunit found in the commercial drug Pegloticase. Next, we sought to determine the average M_n of the PLP on the UOx-PLP conjugate. Notably, we found free PLP was barely degradable by proteinase K even after 48 h incubation (Figure S8), whereas UOx was rapidly degraded within 24 h (Figure 1G, black trace). By harnessing this different degradation rate, we digested UOx-PLP with proteinase K for 48 h, and then analyzed the products with SEC (Figure 1G, red trace). Apart from the typical peaks corresponding to the fragments of degraded UOx (Figure 1G, red and black traces, retention volume of 15.5–20.5 mL), the degraded UOx-PLP also showed an additional peak around the retention volume of 10.0–14.5 mL, which was assigned to be PLP. This PLP peak after UOx-PLP degradation was found to be almost overlaid but slightly broader than the standard PLP_{sk} (Figure 1G, grey trace). Thus, the M_n of PLP on the UOx-PLP was tentatively determined between 3–5 kDa. This notion was further confirmed by examining the intensity at both 280 and 215 nm in the UV spectroscopy of UOx and UOx-PLP (Figure S9), which gave an average M_n of PLP ~3.7 kDa, in good agreement with the above SEC analysis. Matrix-assisted laser desorption/ionization time-of-flight (MALDI-TOF) mass spectrometry was also employed to garner additional insights into the M_n of PLP fragments from the proteinase K-treated UOx-PLP (Figure S10). Peaks assignable to PLP attaching different peptide fragments in the range of 1500–5000 Da were observed. As the ionization and flight of PLP fragments in MALDI are influenced by many factors, it should be noted that the MALDI spectrum cannot faithfully reflect the dispersity of the PLP.

In Vitro Activity and Stability of UOx-PLP

The in vitro activities of the conjugates were examined by the fluorometric assay measured with Amplex red reagent, which revealed ~82% and 71% retention of the original UOx activity for UOx-PLP and PEG-UOx, respectively (Figure 2A). Thermofluor assay (Figure 2B) showed a

slightly increased T_m (78°C) for UOx-PLP compared to UOx (72°C) and PEG-UOx (68°C), suggesting an improved thermostability. Additionally, UOx-PLP was found to retain ~62% of the enzymatic activity after 30 min of heat shock at 70°C. In contrast, UOx and PEG-UOx retained only 30% and 35% of the catalytic activity after the same treatment, respectively (Figure 2C), echoing the conclusion of previous thermofluor assay. As Gibson et al. previously demonstrated the antifreeze capacity of PLP by inhibiting ice crystal growth, we also tested the enzymatic activity of UOx-PLP after freeze-drying and repeated freeze-thaw cycles.^[21] Remarkably, upon reconstitution with double-distilled water, the enzyme activity of freeze-dried UOx-PLP retained ~65%, which was significantly higher than the 29% retention of PEG-UOx (Figure 2D). Furthermore, UOx-PLP showed almost negligible changes in enzyme activity after two repeated freeze-thaw cycles, while UOx and PEG-UOx were found to retain ~62% of the enzymatic activity after the same treatments (Figure 2E). UOx-PLP also displayed enhanced proteolytic stability: UOx-PLP preserved nearly 100% of the activity after 1 h of incubation with trypsin, as compared to ~80% and ~25% activity loss after the same treatment for UOx and PEG-UOx, respectively (Figure 2F).

UOx-PLP Mitigates the Immunogenicity of UOx

The immunogenicity of UOx, PEG-UOx and UOx-PLP were evaluated in Sprague-Dawley (SD) rats with repetitive subcutaneous (s.c.) administrations, and the antisera were acquired before the immunization and one week after each injection. Remarkably, enzyme-linked immunosorbent assay (ELISA) examination of the antisera indicated that UOx-PLP induced almost no detectable anti-UOx IgG or IgM throughout the immunization course, while both UOx and PEG-UOx elicited significantly high levels of anti-UOx antibodies (Figure 3A–B). At the end of the experiments, the anti-UOx IgG titer for the UOx-PLP group was 250 and 30 times lower than that of UOx and PEG-UOx (Figure S11A–B and Figure 3C). Similarly, the levels of anti-polymer IgG and IgM in the UOx-PLP antisera were negligible as compared to those in the UOx-PEG antisera (Figure 3D–E). The titer of anti-PEG IgG in the week 4 PEG-UOx antisera was found to be about 10 times higher than that of anti-PLP IgG in the antisera of UOx-PLP (Figure 3F, Figure S11C–D).

UOx-PLP Showed Minimum Accelerated Blood Clearance (ABC) Effects upon Repetitive Administrations

The presence of these anti-PEG antibodies can lead to mild allergic reactions or even life-threatening anaphylaxis, and can accelerate the clearance of PEG-containing materials from the bloodstream, known as the “accelerated blood clearance” (ABC) effect. To evaluate the in vivo pharmacokinetics (PK) and ABC effects upon repeated injections, UOx and the two conjugates were intravenously (i.v.)

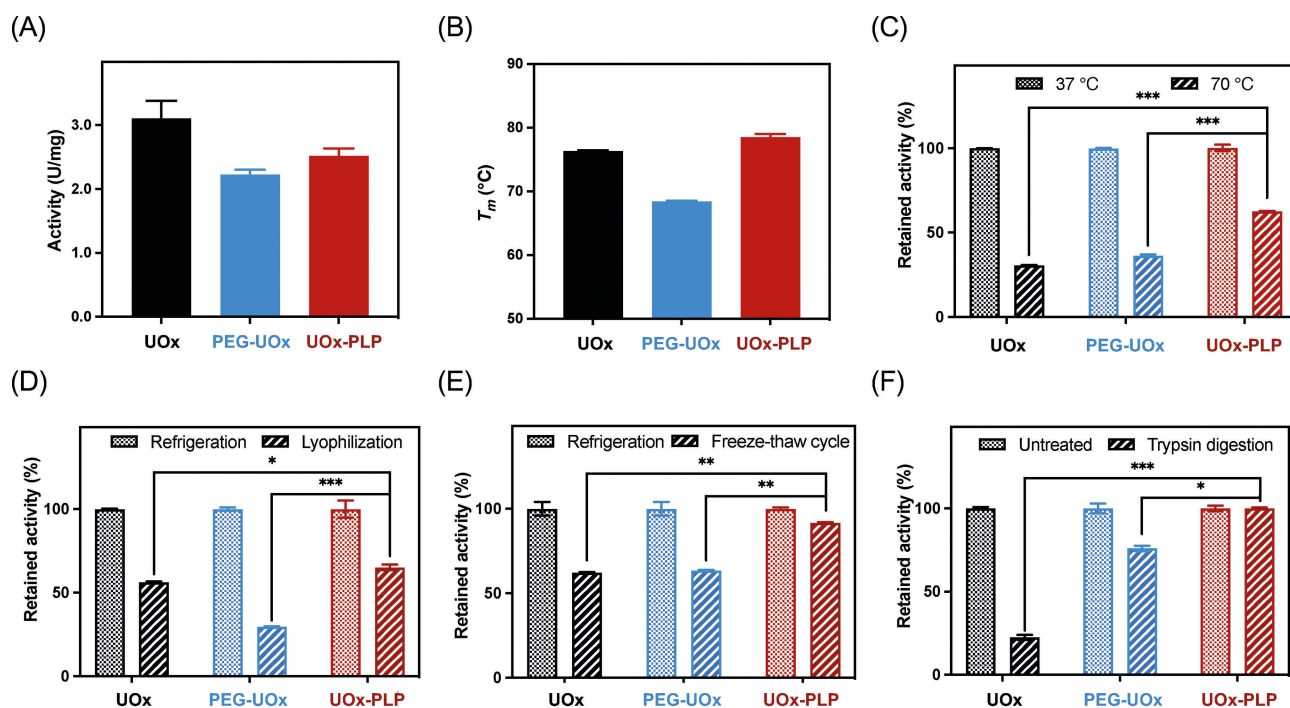


Figure 2. In vitro activity and stability of UOx-PLP. (A) Enzymatic activity of UOx conjugates determined by Amplex Red uric acid/uricase assay kit. (B) Melting temperatures (T_m) of UOx and UOx conjugates measured by thermofluor-based assay. (C) Enzymatic assay of UOx conjugates after incubation at 37 and 70 °C for 0.5 h. (D–E) Enzymatic assay of UOx conjugates after (D) lyophilization and reconstitution, (E) two cycles of freeze-thaw, and (F) trypsin digestion at 37 °C for 1 h. Data are presented as means \pm SD. *P* values are determined by t-test analysis: **P* < 0.05, ***P* < 0.01, ****P* < 0.001.

injected into SD rats for three weeks and the sera at designed time points were collected after the 1st and 3rd administrations (Figure 4A). Besides the conventional dosage groups administrated with consecutive and identical UOx variants, a “cross-dosing” group was also set in which the rats were infused with PEG-UOx for the first two weeks and switched to UOx-PLP for the 3rd week (Figure 4A).

Previous studies have suggested complement activation upon injection of PEGylated proteins or LNP.^[22] For this, we measured the contents of Sc5b-9, the terminal complement complex mutually shared by all three pathways of complement activation. UOx-PLP displayed weaker boost in the concentration of Sc5b-9 at 0 h to 6 h after the first injection than PEG-UOx (Figure 4B–C) and was not significantly different from UOx, suggesting PEG, rather than UOx, stimulated the activity of complement system. Interestingly, the cross-dosing group also displayed lower level of Sc5b-9 after the 3rd injection compared to PEG-UOx. The concentration of Sc5b-9 appeared to peak earlier in the 3rd injection as compared to the 1st injection (Figure 4B–C).

The plasma UOx and uric acid levels at different time points after the 1st and 3rd injections were measured by the Amplex Red uricase and uric acid assay, respectively. For the 1st injection, both PEG-UOx and UOx-PLP showed significantly prolonged PK profiles compared to UOx, with the elimination half-life determined as 31.3, 30.5, and 3.2 h, respectively. No significant difference in PK was found for PEG-UOx and UOx-PLP upon the 1st injection (Figure 4D). Likewise, there was also no difference in the uric acid

knockdown curves for PEG-UOx and UOx-PLP after the 1st injection (Figure 4E). Remarkably, PEG-UOx showed significantly rapid clearance from blood after the 3rd injection (Figure 4F), a clear indication of ABC effect. In contrast, both UOx-PLP and the cross-dosing group gave no sign of ABC effect with the PK profiles almost identical to the 1st injection (Figure 4F). Echoing the PK results, PEG-UOx in the 3rd injection suffered a markable decline in uric acid-eliminating capacity (Figure 4G). In contrast, both UOx-PLP and cross-dosing group reduced the uric acid level in the 3rd injection in a fashion similar to UOx-PLP in its 1st injection (Figure 4G).

Furthermore, the biodistribution of UOx variants was evaluated by quantifying the fluorescence of cyanine5 (Cy5)-labeled UOx conjugates in major organs at 48 h following the 1st and 3rd injections. After the initial injection, PEG-UOx and UOx-PLP demonstrated comparable biodistribution profiles, with the liver exhibiting the highest Cy5 fluorescence for both conjugates. Notably, UOx-PLP presented a slightly higher fluorescence signal compared to PEG-UOx. In contrast, UOx itself was virtually undetectable in all organs (Figure S12A). At 48 h post the 3rd injection, both UOx-PLP and the cross-dosing groups retained the biodistribution pattern and fluorescence intensity observed after the 1st injection (Figure S12B). In contrast, PEG-UOx showed a diminished fluorescent signal after the 3rd injection, suggesting a more rapid clearance from systemic circulation compared to the initial dose.

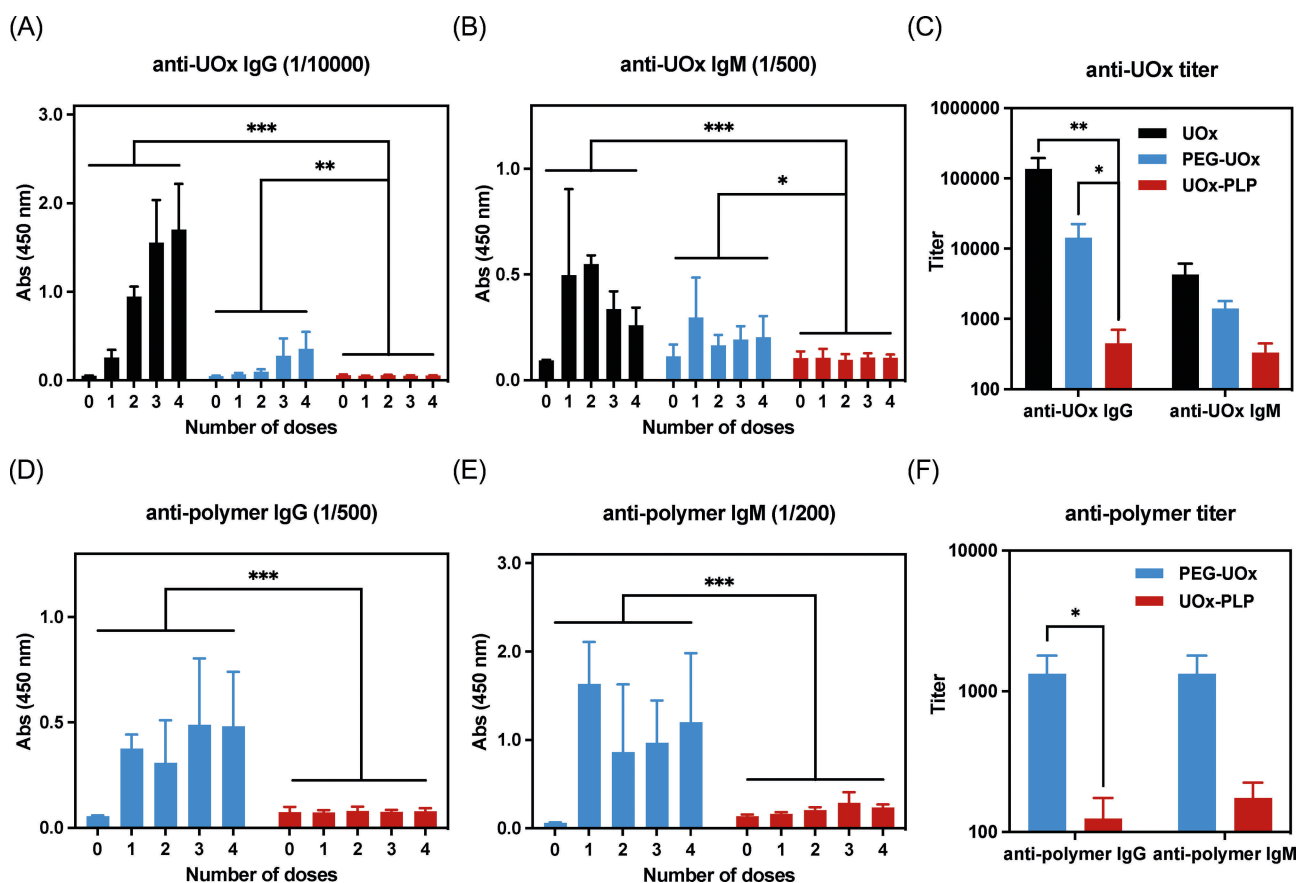


Figure 3. In vivo immunogenicity of UOx, PEG-UOx, and UOx-PLP in SD rats. SD rats ($n=4$) were s.c. injected with UOx variants at a weekly dose of 0.7 mg/kg for 4 weeks; antisera were drawn every week starting from day 0. (A–B) ELISA determination of anti-UOx IgG (A) and IgM (B) contents after each immunization. The plates were coated with UOx and incubated with 10000-fold (for IgG) or 500-fold (for IgM) prediluted antisera. (C) Anti-UOx titers in the antisera drawn from week 4. The antibody titers were determined as the maximum dilution ratio with a signal/noise ratio over 2. (D–E) ELISA determination of anti-polymer IgG (D) and IgM (E) contents after each immunization. For each polymer-of-interest, the plates were coated with the corresponding *N*-terminal specific polymer-interferon conjugate and incubated with 500-fold (for IgG) or 200-fold (for IgM) prediluted sera. (F) Anti-polymer titers in sera drawn from week 4. Data are presented as means \pm SD. *P* values are determined by two-way ANOVA analysis (B–C, E–F) and *t*-test analysis (D, G): * $P < 0.05$, ** $P < 0.01$, *** $P < 0.001$.

UOx-PLP Showed Sustained and Unchanged Efficacy in Knock-Out (*Uox*-KO) Hyperuricemia Mice Model after Repetitive Administrations

We further evaluated the therapeutic performance of UOx-PLP in a UOx knock-out (*Uox*-KO) hyperuricemia mice model lacking endogenous UOx. The model mice have full immune systems and exhibit stable and high blood uric acid levels for more than 20 weeks, allowing long-term evaluations of the impact of immunogenicity on the efficacy of different UOx conjugates. For this, the hyperuricemia mice received five consecutive intraperitoneal (i.p.) dosing of UOx-PLP, PEG-UOx or PBS ($n=3-4$) at 6 U/kg each and the plasma uric acid levels were quantified by ultra performance liquid chromatography-tandem mass spectrometry (UPLC-MS-MS). To avoid uric acid fluctuations caused by stresses from excessive blood drawings, efficacies were monitored from the 3rd injection and thereafter. It was found the plasma uric acid concentrations in the sera of PEG-UOx and UOx-PLP groups were similar throughout the week after the 3rd administration. Six days after the 3rd injection,

the plasma uric acid levels of both UOx conjugate groups were significantly lower than the control group with PBS administration, indicating that the efficacy of both PEG-UOx and UOx-PLP can last for at least 7 days (Figure 5A). Remarkably, the plasma uric acid levels of UOx-PLP group were significantly lower than those in the PEG-UOx group in the week after the 4th injection, indicating a greater efficacy of the former (Figure 5B). This difference in efficacy between UOx-PLP and PEG-UOx became more pronounced in the week after the 5th injection (Figure 5C). Six days after the 5th administration, the plasma uric acid levels in the PEG-UOx group returned to a level comparable to the control PBS group, while the UOx-PLP group gave a significant knockdown concentration of plasma uric acid ($p < 0.006$). Overall, it was found that the efficacy of PEG-UOx in reducing plasma uric acid levels gradually diminished with repeated dosing, as compared to no significant decrease in the efficacy for UOx-PLP with the same dosing regimen (Figure 5A–C). ELISA analysis revealed that both the titers of anti-UOx and anti-polymer antibodies increased gradually upon repeated dosing of

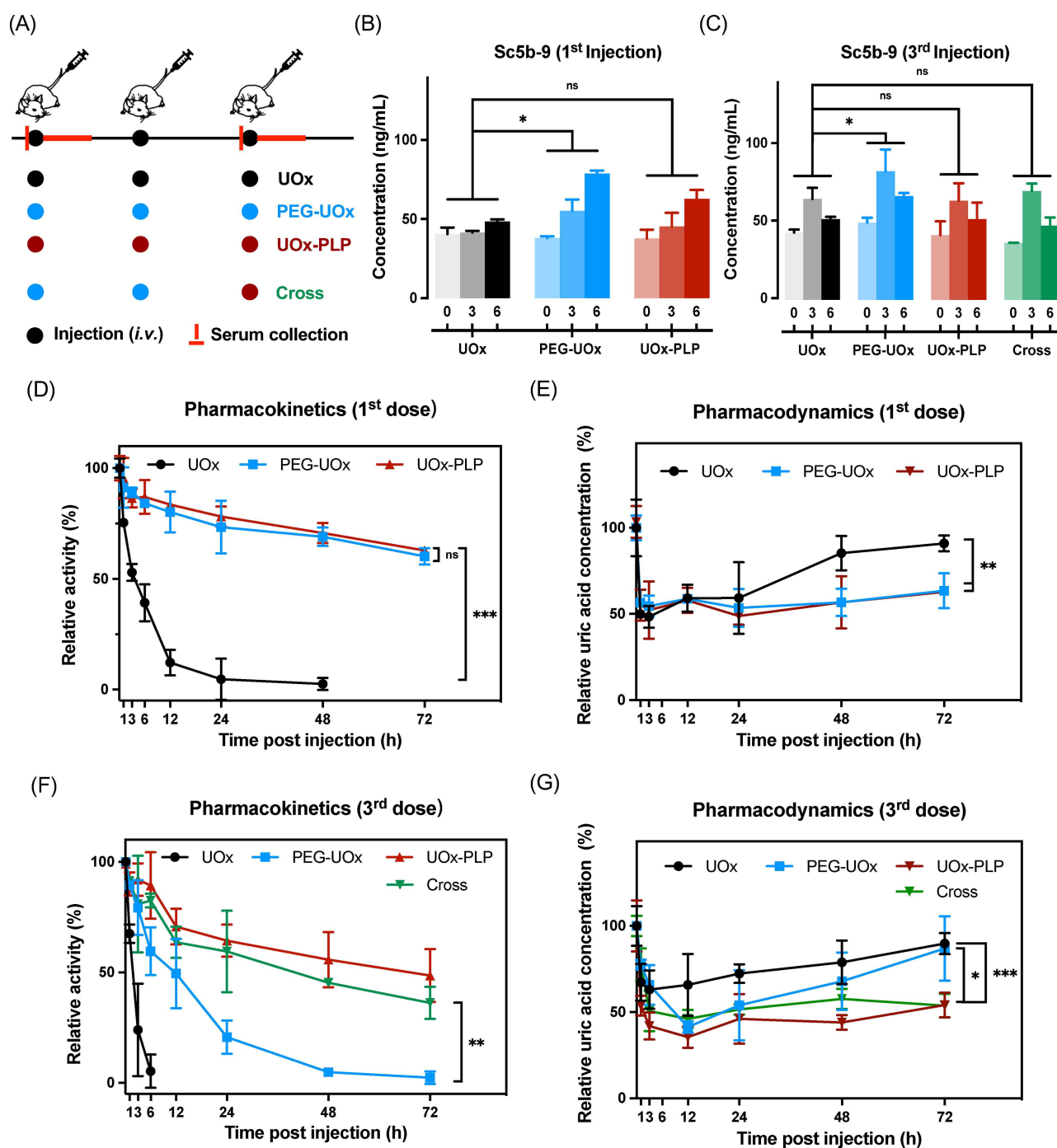


Figure 4. In vivo PK profile and ABC effect evaluation. (A) Schematic illustration of the dosage regimen and antisera collection schedule: SD rats ($n=3$) were i.v. injected with UOx variants at a weekly dose of 15 U/kg for 3 weeks; sera were collected before and at designed time points after the 1st and 3rd administration. (B–C) Terminal complement complex Sc5b-9 contents in 0 h, 3 h and 6 h sera after the (B) 1st and (C) 3rd administrations, respectively. (D, F) The PK profiles, determined by enzyme activity assay, of UOx and different UOx conjugates after the (D) 1st and (F) 3rd administrations. (E, G) The uric acid-eliminating ability of UOx and different UOx conjugates after the (E) 1st and (G) 3rd administrations. Data are presented as means \pm SD. P values are determined by two-way ANOVA analysis: * $P < 0.05$, ** $P < 0.01$, *** $P < 0.001$.

PEG-UOx, with a significant boost after the 4th injection (Figure 5D–G). In contrast, the antibody titers in the UOx-PLP group showed minimal increase over time (Figure 5D–G). Taken together, the results suggested a strong association of the ADA generation with the efficacy loss for

the PEG-UOx group. Also, no significant loss in weight was observed for all mice (Figure S13). Blood biochemistry analysis showed no sign of liver or kidney injury (Figure S14). The excellent biosafety profile of all UOx variants was illustrated by the histological examination of the

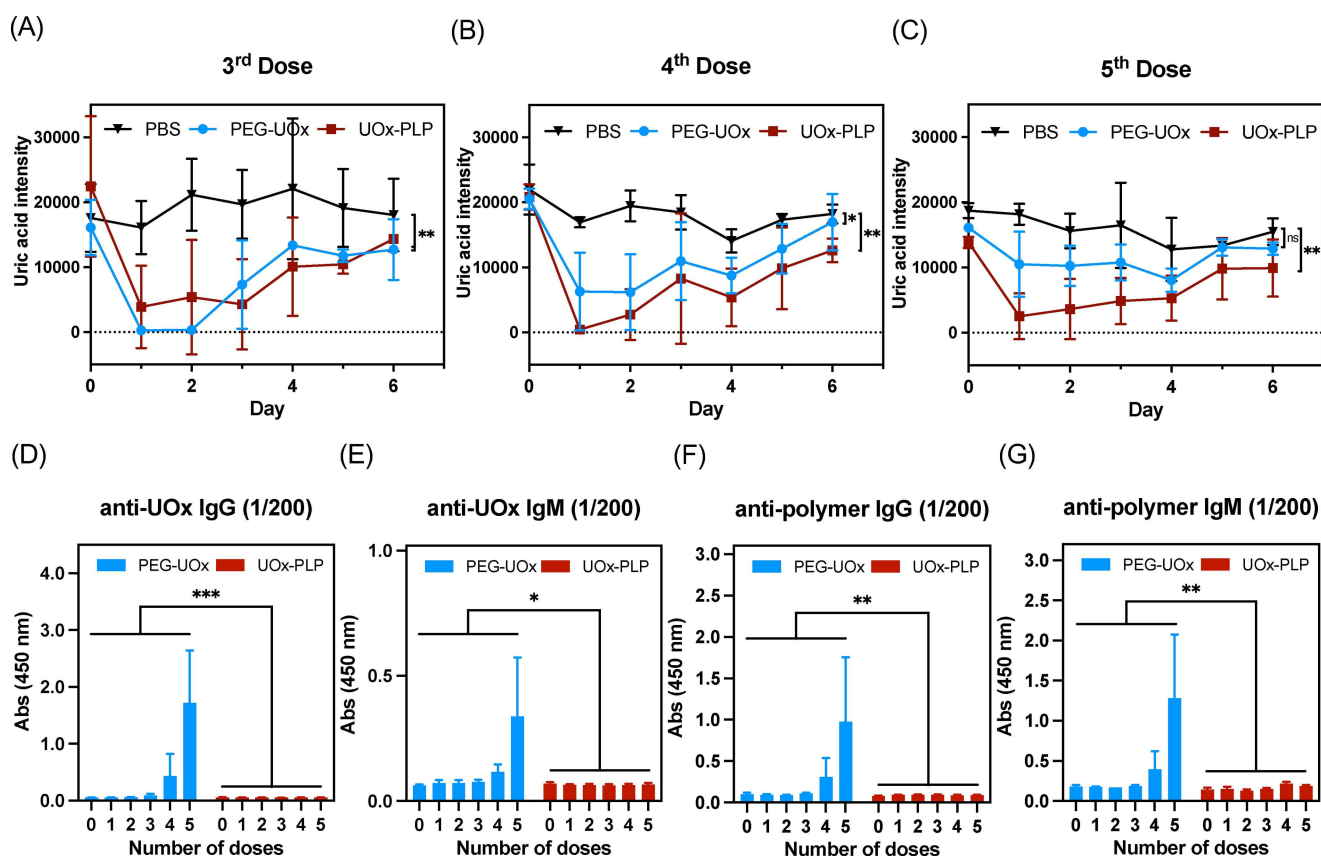


Figure 5. In vivo therapeutic performance in UOx knock-out (*Uox-KO*) hyperuricemia model mice. Model mice ($n=3-4$ per group) were intraperitoneal (i.p.) injected with UOx conjugates or PBS at a weekly dose of 6 U/kg for 5 weeks; Plasma was collected every day during treatment. (A–C) Plasma uric acid quantification by UPLC-MS-MS in UOx conjugates group after the 3rd (A), 4th (B) and 5th (C) administration. (D–G) ELISA analysis of plasma antibody level after each administration. Anti-UOx IgG (D), IgM (E) and anti-polymer IgG (F), IgM (G) contents were determined by the method as described above. Data are presented as means \pm SD. *P* values are determined by two-way ANOVA analysis: **P* < 0.05, ***P* < 0.01, ****P* < 0.001.

dissected organ sections, which showed no major damage in the liver, spleen, and kidney (Figure S15).

Repetitive Injection Toxicity of Free PLP Polymers

The repeat-dose toxicity of PLP was examined in SD rats. Briefly, PBS and PLP of different M_n (2.5, 5, and 10 kDa, namely PLP₂₅, PLP₅₀, and PLP₁₀₀, respectively, Figure S16) were individually injected into SD rats via the tail vein at a weekly dose of 30 mg/kg (roughly 50 times higher than regular dose in efficacy study) for totally 12 weeks. No death nor significant differences showed in body weight (Figure 6A). Examination of the organ weights showed no sign of liver or kidney dysfunction for rats receiving one week after the last administration (Figure 6B). Blood biochemical (Figure S17) and complete blood count (Figure S18) were found in normal ranges for all groups. Finally, Immunohistochemistry of the hematoxylin-eosin (H&E)-stained sections of major organs showed no signs of organ damage (Figure 6C). Of note, repetitive administration of PEG at high dosages is well-known to cause significant vacuolation in the kidneys and spleen.^[23]

Conclusion

For immunogenic proteins like UOx, high modification degree to fully cover the epitope on its surface is vital to achieve the desired protection. By using the grafting-from approach, and adding a competitive inhibitor of UOx to transiently block the catalytic center during the polymerization, we successfully solved the problem and achieved facile preparation of UOx-PLP conjugate with high PLP density (~ 13.8 strands per subunit) and minimum loss of the pristine enzyme activity ($\sim 82\%$ preserved activity). The high efficiency and simplicity of method allowed the synthesis to be completed in a single step and within 5 min. Also, we established a comprehensive and semi-quantitative characterization protocol to better determine the key structural characters of the conjugates. The modification of PLP was found to impart UOx with enhanced thermal, frozen, freeze-thaw, and proteolytic stabilities. As Pegloticase was supplied in saline buffer, the superior ability of UOx-PLP in withstanding lyophilization may allow it to be supplied as powder with reduced storage and transportation costs abandoning cold-chain, although further optimization is needed.

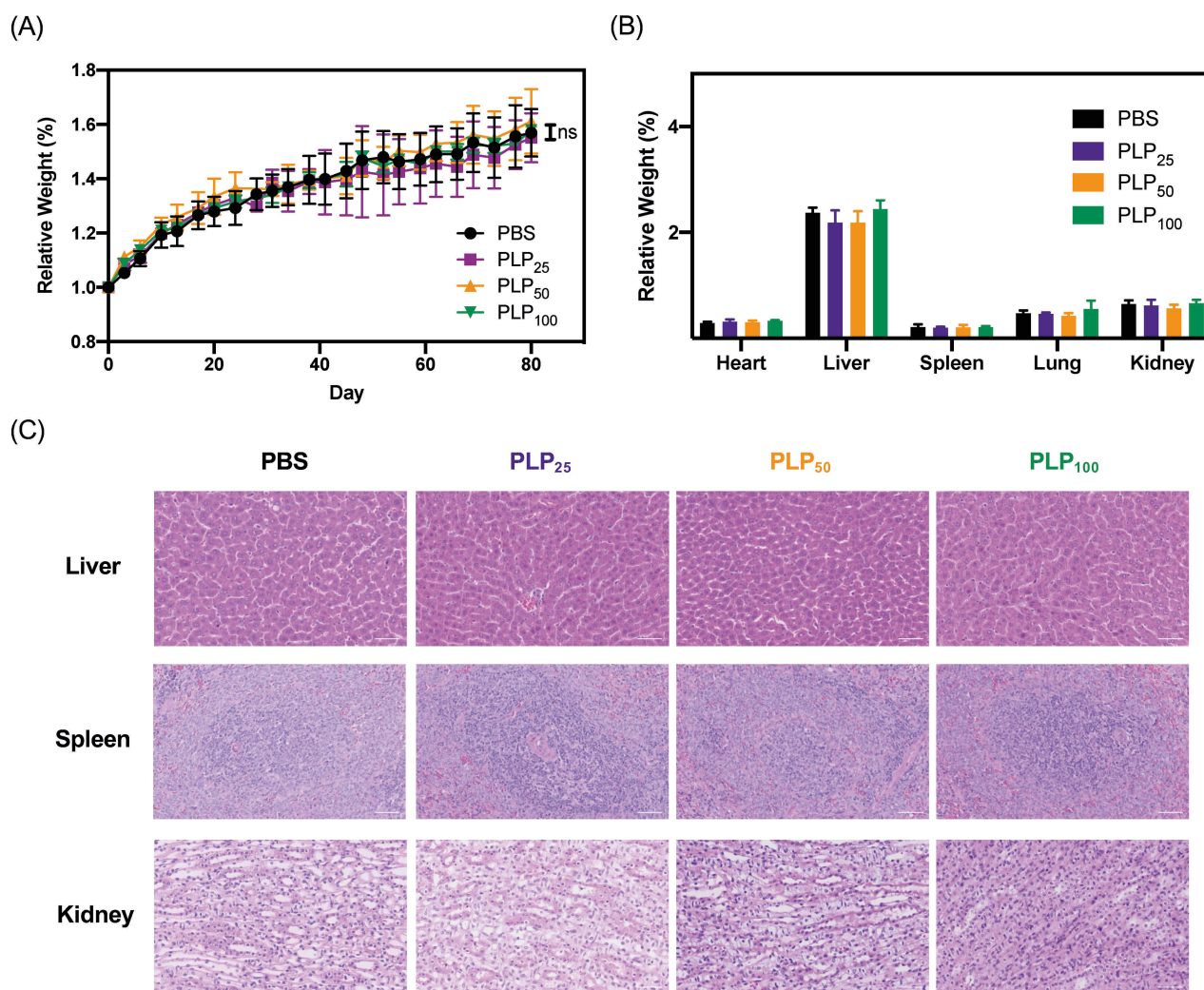


Figure 6. Repeat-dose toxicity of PLP polymers. (A) Change of body weight over 12 weeks for the rats receiving PBS or PLP with different M_n . (B–C) Comparison of (B) weights and (C) H&E-stained sections of major organs of the rats receiving PBS or PLP for 12 weeks. PBS and PLP were injected into SD rats via the tail vein at a weekly dose of 30 mg/kg repeating for 12 weeks. Data are expressed as mean \pm SD ($n=4$).

It should be noted that the PEG-UOx conjugate prepared for this study closely mirrors the performance of the commercial drug Pegloticase (e.g. modification degree, circulation half-life, enzymatic activity, etc.), making it a practical and legitimate control group for comparison. Our results found UOx-PLP elicited almost no anti-UOx/anti-polymer antibodies and gave no sign of ABC effect after repetitive immunizations in SD rats, which outperformed PEG-UOx in side-by-side comparison. Moreover, the PK profile of UOx-PLP remained unchanged after cross-administrating to rats previously received two doses of PEG-UOx and already with high titers of both anti-UOx and anti-PEG antibodies in the sera. The measured plasma uric acid levels in the cross-dosing group were almost identical to the UOx-PLP group, again underscoring the improved efficacy of UOx-PLP over PEG-UOx upon repeated administration (Figure 4E, G). The above result highlighted the excellent ability of PLP in shielding UOx epitopes, and implying potential effectiveness of using UOx-PLP even in patients who have already received and developed ADA to PEG-

UOx. Finally, the therapeutic performance of UOx-PLP was further demonstrated in a *Uox*-KO hyperuricemia model, which showed almost no loss of efficacy even after five repeated administrations, whereas PEG-UOx experienced steady efficacy loss upon continuous administrations.

Based on the above results, we have coined a preliminary, simplified “nanourchin” model to interpret the performance of the UOx-PLP and the difference with PEG-UOx (Figure 7). The key hypothesis of this model is the high-density, rigid spike-like PLP generated a dense layer of physical barrier for better protection of UOx than the flexible hair-like PEG. Such an array of rigid rod PLP outer layer repelled and prevented the direct contact of UOx-PLP with protease, antibodies, and various immune cells (Figure 7A). For PEG-UOx with the flexible PEG outer layer, however, biomacromolecules and cells can still propel and generate immune synapses, eventually stimulating immune responses (Figure 7B). The superior proteolytic stability of UOx-PLP over PEG-UOx is a vivid demonstration of this simplified model (Figure 2F). Importantly, small molecules

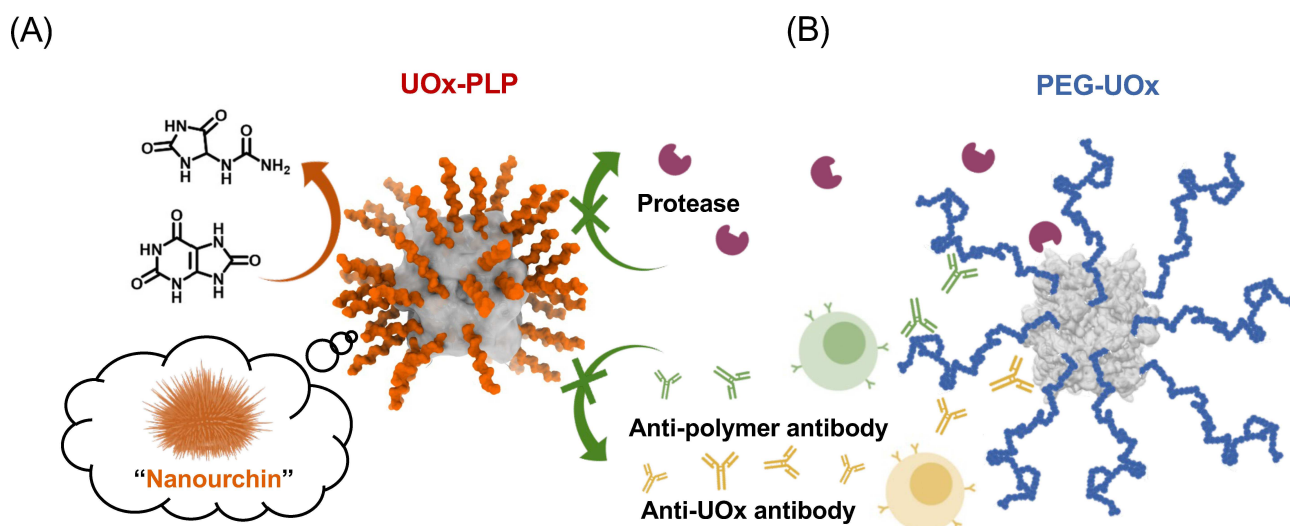


Figure 7. Schematic illustration of “nanourchin” model and different in vivo performances between UOx-PLP (A) and PEG-UOx (B).

such as the substrate of UOx can still penetrate this physical barrier of UOx-PLP and diffuse into the catalytic center easily, allowing the conjugate for uric acid elimination. Overall, the simple preparation and outstanding nonclinical results highlight the enormous potential of UOx-PLP for future clinical translation and the generality of the grafting-from method may shed light on the development of other therapeutic proteins, particularly enzymes.

Notes

The authors declare no competing financial interest. A PCT patent application has been filed partially based on this work with R.C.Z and H.L. as coinventors.

Acknowledgements

This work was supported by Beijing Natural Science Foundation (Z220023), the National Key Research and Development Program of China (2019YFA0904203), National Natural Science Foundation of China (22125101), National Key Research and Development Program of China (2019YFA0904100), Shenzhen Science and Technology Program (KJZD20230923115906013), and SIAT Distinguished Young Scholars (E4G021).

Conflict of Interest

The authors declare no conflict of interest.

Data Availability Statement

The data that support the findings of this study are available in the supplementary material of this article.

Keywords: protein-polymer conjugates · polyproline · immune response · uricase · hyperuricemia

- [1] a) M. Aringer, J. Graessler, *Lancet* **2008**, 372, 1929–1930; b) M. Dehlin, L. Jacobsson, E. Roddy, *Nat. Rev. Rheumatol.* **2020**, 16, 380–390.
- [2] a) GBD 2021 Gout Collaborators, *Lancet Rheumatol.* **2024**, 6, e507–e517; b) Y. Hao, H. Li, Y. P. Cao, Y. W. Chen, M. Y. Lei, T. Y. Zhang, Y. Xiao, B. Y. Chu, Z. Y. Qian, *J. Biomed. Nanotechnol.* **2019**, 15, 951–965.
- [3] a) T. J. Major, N. Dalbeth, E. A. Stahl, T. R. Merriman, *Nat. Rev. Rheumatol.* **2018**, 14, 341–353; b) N. Dalbeth, A. Phipps-Green, C. Frampton, T. Neogi, W. J. Taylor, T. R. Merriman, *Ann. Rheum. Dis.* **2018**, 77, 1048–1052.
- [4] a) C. W. Qi, U. U. M. Nordin, S. Mahmood, N. R. Karusan, R. Khalid, N. Nordin, C. Fornaguera, N. Ahmad, *ACS Appl. Nano Mater.* **2024**, 7, 9816–9846; b) T. B. Friedman, G. E. Polanco, J. C. Appold, J. E. Mayle, *Comp. Biochem. Physiol. B.* **1985**, 81, 653–659.
- [5] a) D. Concolino, F. Deodato, R. Parini, *Ital. J. Pediatr.* **2018**, 44, 120; b) N. Schlesinger, F. Perez-Ruiz, F. Liote, *Nat. Rev. Rheumatol.* **2023**, 19, 640–649; c) X. P. Liu, Z. J. Zhang, Y. Zhang, Y. J. Guan, Z. Liu, J. S. Ren, X. G. Qu, *Adv. Funct. Mater.* **2016**, 26, 7921–7928.
- [6] P. M. Navolanic, C. H. Pui, R. A. Larson, M. R. Bishop, T. E. Pearce, M. S. Cairo, S. C. Goldman, S. C. Jeha, C. B. Shanholtz, J. P. Leonard, J. A. McCubrey, *Leukemia* **2003**, 17, 499–514.
- [7] K. C. Allen, A. H. Champlain, J. A. Cotliar, S. M. Belknap, D. P. West, J. Mehta, S. M. Trifilio, *Drug Saf.* **2015**, 38, 183–187.
- [8] a) N. Schlesinger, U. Yasothan, P. Kirkpatrick, *Nat Rev Drug Discov* **2011**, 10, 17–18; b) M. K. Reinders, T. L. T. A. Jansen, *Ther. Clin. Risk Manag.* **2010**, 6, 543–550.
- [9] a) M. R. Sherman, M. G. Saifer, F. Perez-Ruiz, *Adv. Drug Deliv. Rev.* **2008**, 60, 59–68; b) J. S. Sundy, H. S. Baraf, R. A. Yood, N. L. Edwards, S. R. Gutierrez-Urena, E. L. Treadwell, J. Vazquez-Mellado, W. B. White, P. E. Lipsky, Z. Horowitz, W. Huang, A. N. Maroli, R. W. Waltrip, 2nd, S. A. Hamburger, M. A. Becker, *JAMA* **2011**, 306, 711–720.

- [10] P. E. Lipsky, L. H. Calabrese, A. Kavanaugh, J. S. Sundy, D. Wright, M. Wolfson, M. A. Becker, *Arthritis Res. Ther.* **2014**, *16*, R60.
- [11] a) N. J. Ganson, S. J. Kelly, E. Scarlett, J. S. Sundy, M. S. Hershfield, *Arthritis Res. Ther.* **2006**, *8*, R12; b) M. S. Hershfield, N. J. Ganson, S. J. Kelly, E. L. Scarlett, D. A. Jagers, J. S. Sundy, *Arthritis Res. Ther.* **2014**, *16*, R63.
- [12] a) J. J. Verhoef, J. F. Carpenter, T. J. Anchordoquy, H. Schellekens, *Drug Discov. Today* **2014**, *19*, 1945–1952; b) P. Zhang, F. Sun, S. Liu, S. Jiang, *J. Control. Release* **2016**, *244*, 184–193.
- [13] a) Y. Ju, W. S. Lee, E. H. Pilkington, H. G. Kelly, S. Y. Li, K. J. Selva, K. M. Wragg, K. Subbarao, T. H. O. Nguyen, L. C. Rowntree, L. F. Allen, K. Bond, D. A. Williamson, N. P. Truong, M. Plebanski, K. Kedzierska, S. Mahanty, A. W. Chung, F. Caruso, A. K. Wheatley, J. A. Juno, S. J. Kent, *ACS Nano* **2022**, *16*, 11769–11780; b) A. W. Richter, E. Akerblom, *Int. Arch. Allergy Appl. Immunol.* **1984**, *74*, 36–39; c) B. M. Chen, Y. C. Su, C. J. Chang, P. A. Burnouf, K. H. Chuang, C. H. Chen, T. L. Cheng, Y. T. Chen, J. Y. Wu, S. R. Roffler, *Anal. Chem.* **2016**, *88*, 10661–10666; d) B. M. Chen, T. L. Cheng, S. R. Roffler, *ACS Nano* **2021**, *15*, 14022–14048.
- [14] a) E. M. Pelegri-O'Day, E. W. Lin, H. D. Maynard, *J. Am. Chem. Soc.* **2014**, *136*, 14323–14332; b) K. M. Burrige, R. C. Page, D. Konkolewicz, *Polymer* **2020**, *211*, 123062; c) C. J. Chen, D. Y. W. Ng, T. Weil, *Prog. Polym. Sci.* **2020**, *105*, 101241; d) A. J. Russell, S. L. Baker, C. M. Colina, C. A. Figg, J. L. Kaar, K. Matyjaszewski, A. Simakova, B. S. Sumerlin, *Aiche J.* **2018**, *64*, 3230–3245; e) U. Binder, A. Skerra, *Curr. Opin. Colloid In.* **2017**, *31*, 10–17; f) Z. F. Yuan, B. W. Li, L. Q. Niu, C. J. Tang, P. McMullen, P. Jain, Y. W. He, S. Y. Jiang, *Angew. Chem. Int. Ed.* **2020**, *59*, 22378–22381; g) V. Schellenberger, C. W. Wang, N. C. Geething, B. J. Spink, A. Campbell, W. To, M. D. Scholle, Y. Yin, Y. Yao, O. Bogin, J. L. Cleland, J. Silverman, W. P. C. Stemmer, *Nat. Biotechnol.* **2009**, *27*, 1186–1190; h) S. K. Zhang, Y. Z. Sun, L. S. Zhang, F. Zhang, W. P. Gao, *Adv. Sci.* **2023**, *10*, 2300469; i) M. Liu, P. Johansen, F. Zabel, J. C. Leroux, M. A. Gauthier, *Nat. Commun.* **2014**, *5*, 5526; j) I. Ozer, G. Kelly, R. P. Gu, X. H. Li, N. Zakharov, P. Sirohi, S. K. Nair, J. H. Collier, M. S. Hershfield, A. M. Hucknall, A. Chilkoti, *Adv. Sci.* **2022**, *9*, 2103672; k) M. Tully, M. Dimde, C. Weise, P. Pouyan, K. Licha, M. Schirner, R. Haag, *Biomacromolecules* **2021**, *22*, 1406–1416; l) T. X. Viegas, M. D. Bentley, J. M. Harris, Z. F. Fang, K. Yoon, B. Dizman, R. Weimer, A. Mero, G. Pasut, F. M. Veronese, *Bioconjugate Chem.* **2011**, *22*, 976–986; m) B. W. Li, P. Jain, J. R. Ma, J. K. Smith, Z. F. Yuan, H. C. Hung, Y. W. He, X. J. Lin, K. Wu, J. Pfaendtner, S. Y. Jiang, *Sci. Adv.* **2019**, *5*, eaaw9562; n) X. F. Han, Y. Lu, J. B. Xie, E. S. Zhang, H. Zhu, H. Du, K. Wang, B. Y. Song, C. B. Yang, Y. J. Shi, Z. Q. Cao, *Nat. Nanotechnol.* **2020**, *15*, 605–614; o) P. Zhang, P. Jain, C. Tsao, Z. F. Yuan, W. C. Li, B. W. Li, K. Wu, H. C. Hung, X. J. Lin, S. Y. Jiang, *Angew. Chem. Int. Ed.* **2018**, *57*, 7743–7747; p) Y. L. Hu, Y. Q. Hou, H. Wang, H. Lu, *Bioconjugate Chem.* **2018**, *29*, 2232–2238; q) Y. Q. Hou, Y. Zhou, H. Wang, R. J. Wang, J. S. Yuan, Y. L. Hu, K. Sheng, J. Feng, S. T. Yang, H. Lu, *J. Am. Chem. Soc.* **2018**, *140*, 1170–1178; r) A. Birke, J. Ling, M. Barz, *Prog. Polym. Sci.* **2018**, *81*, 163–208; s) C. K. Fu, B. Demir, S. Alcantara, V. Kumar, F. Han, H. G. Kelly, X. Tan, Y. Yu, W. Z. Xu, J. C. Zhao, C. Zhang, H. Peng, C. Boyer, T. M. Woodruff, S. J. Kent, D. J. Searles, A. K. Whittaker, *Angew. Chem. Int. Ed.* **2020**, *59*, 4729–4735; t) H. Sánchez-Morán, J. L. Kaar, D. K. Schwartz, *J. Am. Chem. Soc.* **2024**, *146*, 9112–9123.
- [15] a) X. P. Zhang, W. Chen, X. Y. Zhu, Y. F. Lu, *ACS Appl. Mater. Inter.* **2017**, *9*, 7972–7978; b) X. Zhang, D. Xu, X. Jin, G. Liu, S. Liang, H. Wang, W. Chen, X. Zhu, Y. Lu, *J. Control. Release* **2017**, *255*, 54–61; c) P. Zhang, F. Sun, C. Tsao, S. J. Liu, P. Jain, A. Sinclair, H. C. Hung, T. Bai, K. Wu, S. Y. Jiang, *Proc. Natl. Acad. Sci. U.S.A.* **2015**, *112*, 12046–12051; d) B. Li, Z. Yuan, P. Zhang, A. Sinclair, P. Jain, K. Wu, C. Tsao, J. Xie, H. C. Hung, X. Lin, T. Bai, S. Jiang, *Adv. Mater.* **2018**, *30*, e1705728; e) S. Liang, Y. Liu, X. Jin, G. Liu, J. Wen, L. L. Zhang, J. Li, X. B. Yuan, I. S. Y. Chen, W. Chen, H. Wang, L. Q. Shi, X. Y. Zhu, Y. F. Lu, *Nano Res.* **2016**, *9*, 1022–1031.
- [16] a) Z. L. Ban, M. D. Sun, H. H. Ji, Q. X. Ning, C. X. Cheng, T. F. Shi, M. H. He, X. N. Chen, H. F. Lu, X. He, C. Y. Guo, Y. He, D. Shao, Y. He, *J. Control. Release* **2024**, *372*, 862–873; b) M. J. Zhang, A. Hussain, B. Hu, H. Y. Yang, C. H. Li, S. Guo, X. F. Han, B. Li, Y. L. Dai, Y. H. Cao, H. Chi, Y. H. Weng, C. F. Qin, Y. Y. Huang, *Nat. Commun.* **2024**, *15*, 6463.
- [17] a) I. Ozer, G. Kelly, R. P. Gu, X. H. Li, N. Zakharov, P. Sirohi, S. K. Nair, J. H. Collier, M. S. Hershfield, A. M. Hucknall, A. Chilkoti, *Adv. Sci.* **2022**, *9*, 2103672; b) P. Zhang, F. Sun, S. Liu, S. Jiang, *J. Control. Release* **2016**, *244*, 184–193.
- [18] a) Y. Hu, Z. Y. Tian, W. Xiong, D. Wang, R. Zhao, Y. Xie, Y. Q. Song, J. Zhu, H. Lu, *Natl. Sci. Rev.* **2022**, *9*, nwc033; b) M. Badreldin, R. Le Scouarnec, S. Lecommandoux, S. Harrison, C. Bonduelle, *Angew. Chem. Int. Ed.* **2022**, *61*, e202209530; c) E. Tinajero-Díaz, N. Judge, B. Li, T. Leigh, R. D. Murphy, P. D. Topham, M. J. Derry, A. Heise, *ACS Macro Lett.* **2024**, *13*, 1031–1036; d) H. Beausery, C. Grazon, S. Antoine, M. Badreldin, P. Salas-Ambrosio, S. Harrison, E. Garanger, S. Lecommandoux, C. Bonduelle, *Macromol. Rapid Commun.* **2024**, *45*, 2400079; e) N. Judge, P. G. Georgiou, A. Bissoyi, A. Ahmad, A. Heise, M. I. Gibson, *Biomacromolecules* **2023**, *24*, 2459–2468.
- [19] a) M. T. Ruggiero, J. Sibik, R. Orlando, J. A. Zeitler, T. M. Korter, *Angew. Chem. Int. Ed.* **2016**, *55*, 6877–6881; b) N. Sengupta, S. Padmanaban, S. Dutta, *J. Biol. Chem.* **2023**, *299*, 104589.
- [20] O. Nwajiobi, A. K. Verma, M. Raj, *J. Am. Chem. Soc.* **2022**, *144*, 4633–4641.
- [21] B. Graham, T. L. Bailey, J. R. J. Healey, M. Marcellini, S. Deville, M. I. Gibson, *Angew. Chem. Int. Ed.* **2017**, *56*, 15941–15944.
- [22] a) N. E. Elsadek, A. S. Abu Lila, T. Ishida, in *Polymer-Protein Conjugates*, Chpt. 5 (Eds.: G. Pasut, S. Zalipsky), Elsevier, Amsterdam, **2020**, pp. 103–123; b) A. Gabizon, J. Szebeni, *ACS Nano* **2020**, *14*, 7682–7688.
- [23] J. Sun, J. Chen, Y. Sun, Y. Hou, Z. Liu, H. Lu, *Bioact. Mater.* **2024**, *32*, 333–343.

Manuscript received: December 30, 2024

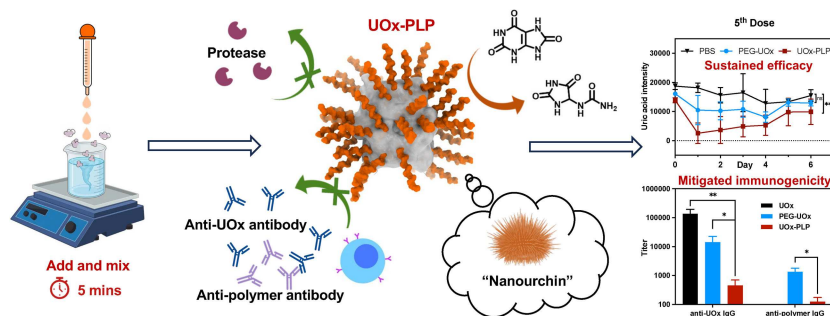
Version of record online: ■■■, ■■■

Forschungsartikel

Biomaterials

R. Zhao, Y. Zhang, B. Ruan, H. Zhang,
N. Lv, J. Li, Y. R. Yang,* X. Luo,*
H. Lu* [e202425559](#)

Nanourchin-like Uricase-Poly(L-proline)
Conjugate with Retained Enzymatic Activity,
Mitigated Immunogenicity, and Sustained
Efficacy Upon Repeated Administrations



Poly(L-proline) conjugated uricase was
facilely produced via a grafting-from
approach, which showed mitigated im-

munogenicity and preserved activity in
vivo after repeated injections.